

**AGNIESZKA KOWALSKA**  
**AGNIESZKA STOBIECKA**  
Institute of General Food Chemistry,  
Faculty of Biotechnology and Food Sciences,  
Technical University of Lodz

## **THE THEORETICAL STUDY ON THE MOLECULAR STRUCTURE AND ELECTRONIC PROPERTIES OF HARMANE**

Review: **Professor Stanisław Wysocki, Ph. D., D. Sc.**

*In this study the geometry optimization of harmane using the semi-empirical (AM1, PM3, MNDO,) ab initio HF as well as the B3LYP method was performed. The calculated geometrical parameters of harmane were compared with the available crystallographic data to verify the extent to which theoretical models approximate the molecular structure of this compound. Additionally, some electronic properties of harmane in the neutral and monocationic form were calculated using various theoretical methods. The semi-empirical ZINDO-1 and TD/B3LYP calculations were carried out using the B3LYP/6-31+G(d,p) optimized geometry of harmane. The utility of the applied methods to predict properties of electronic transitions to the lowest excited singlet states of harmane was discussed.*

### **1. Introduction**

Harmane (1-methyl-9-H-pyrido-[3,4-b] indole) (Fig. 1) belongs to the group of  $\beta$ -carboline alkaloids, which are the compounds of particular interest in the pharmacological science.  $\beta$ -carbolines are known from their biological activity as the central nervous system stimulants, hallucinogens [1-5]. These compounds also exhibit cytotoxic and mutagenic or co-mutagenic properties. Moreover  $\beta$ -carbolines may interact with the double stranded DNA and single stranded RNA [6].

Harmine is composed of a  $\pi$ -deficient pyridine ring fused to a  $\pi$ -sufficient indole ring. The presence of pyrrolic and pyridinic nitrogen atoms in the betacarboline ring allows harmine to act as a hydrogen bond donor / acceptor molecule. Due to a bifunctional hydrogen bonding character of harmine ring, this compound is able to act through hydrogen bonding with variety of solvents too [7,8]. Additionally, its photophysical properties are sensitive to the pH of surrounding medium. Depending on the pH value, in aqueous solutions, harmine may exist as four different species: as a neutral, a monocationic (in which the pyridinic N is protonated), an anionic form or as a zwitterion [9].

Due to the interesting photophysical properties of  $\beta$ -carbolines and their potential pharmacological application as the antidepressants and antitumor drugs, the experimental and theoretical information about the molecular structure of these compounds is vital. The crystal structure of harmine (as a free base) was determined by X-ray diffraction and reported by El-Sayed and co-workers [10]. The geometrical parameters of harmine were also collected in The Cambridge Crystallographic Database [11].

In a few recent years advances in computational hardware and technology have made it possible that existing chemical theories may be applied to more and more complex systems. Therefore theoretical methods are increasingly applied by chemists in variety of problems, for example to predict structural and electronic properties of molecules, to examine solvent effects, to study molecular interactions and even to model excited or transition states of reactions. For this purpose various computational methods may be used, from semi-empirical to very sophisticated and advanced models in which electron correlation is taken into account. Nevertheless, the starting point for all mentioned calculations is to determine the most accurate structure of the molecule. The most accurate geometry of the molecule is defined as having the lowest possible energy (and is determined as the result of geometry optimization or energy minimization). The optimized geometry of a molecule is roughly dictated by the starting positions of the atoms as chosen by the theoretician, therefore the optimized geometrical parameters should be compared with the experimental data. Moreover the calculations refer to an isolated single molecule, whereas measured properties reflect thermal averaging possibly over all the stereoisomers, tautomers of a given compound, which may be structurally quite different from the idealized model system. Therefore care must be taken when comparing calculated and experimental structural properties of the molecule. Once the well-defined (the accurate) geometry of a molecule is determined, chemical properties for a single molecule may be calculated. Typical example of these properties are spectral quantities such as electronic energy and oscillator strengths of the electronic transitions to the lowest excited singlet states for a given molecule [12]. Theoretical calculations have proved to be useful tool in the prediction of the structural and electronic properties, as well as the reactivity of a great number of conjugated systems, including  $\beta$ -carbolines.

The theoretical studies on  $\beta$ -carboline with the use of computational methods have been extensively reported in the literature. These studies have mainly focused on:

- the semi-empirical analysis of structural properties and potential reactivity of  $\beta$ -carboline [13,14,15];
- the semi-empirical prediction of energies and oscillator strengths for electronic transitions in  $\beta$ -carboline in the gaseous phase [16];
- the reproduction of proton affinities of 3-substituted  $\beta$ -carboline including solvent effects with the PCM model [17];
- the protonation and deprotonation processes of pyridoindoles (including  $\beta$ -carboline and their derivatives) [18];
- the excited state proton-transfer tautomerism of  $\beta$ -carboline mediated by hydrogen-bonded complexes [19]
- the determination of  $pK_a$ , lipophilicity, water solubility and polar surface area of harmaline [20].

In the current work we performed the quantum-mechanical study on the molecular structure and electronic properties of harmaline, too. However, beside semi-empirical and HF methods, the theoretical calculations were also performed at the B3LYP level of theory. The calculated using various computational methods structural parameters of neutral form of harmaline were compared with available experimental data. Moreover, the values of the HOMO-LUMO energy were calculated attempting to find a theoretical approach useful in the interpretation of the absorption spectra of harmaline.

Due to the interesting, individual photophysical properties of harmaline monocation, which is used as the fluorescence standard, the calculations were also performed for the protonated form of the compound under study. Additionally, the geometrical changes resulting from protonation of the pyridinic nitrogen of harmaline was discussed. Furthermore, the ZINDO-1 and TD (B3LYP)/6-31+G(d,p) methods were used in this work in order to test their utility to predict the spectroscopic properties of the electronic transitions to the lowest excited singlet states for both neutral and cationic form of harmaline.

## 2. Computational methods

Geometry optimization of neutral and monocationic form of harmaline *in vacuo* was performed at the semi-empirical MNDO, AM1, (Austin Model 1) and PM3 (Parameterized Model) level. The energy minimization calculations were also performed applying Hartree-Fock (HF) and hybrid density functional theory B3LYP methods with the use of 6-31G(d) basis set. In order to determine the influence of polarized and diffuse functions on the predicted properties of harmaline, geometry optimizations with 6-31+G (d,p) basis set were also

performed. Additionally, to verify whether the optimized structures correspond to the energy minimum, diagonalization of the energy second-derivative matrix (Hessian) have been carried out. It was found that there were no negative vibrational frequencies, which indicated that all the optimized structures were at the energy minimum.

The oscillator strengths and the energies of the lowest singlet-singlet electronic transitions have been obtained by ZINDO-1 semi-empirical and time-dependent TD/B3LYP methods using the B3LYP/6-31+G (d,p) optimized geometries of harmane. All calculations were performed with the use of Gaussian 03 suite of programs.

### 3. Results and discussion

#### 3.1. The ground state geometry of neutral form of harmane

The calculated molecular structure and the atom numbering of harmane is presented in Fig. 1.

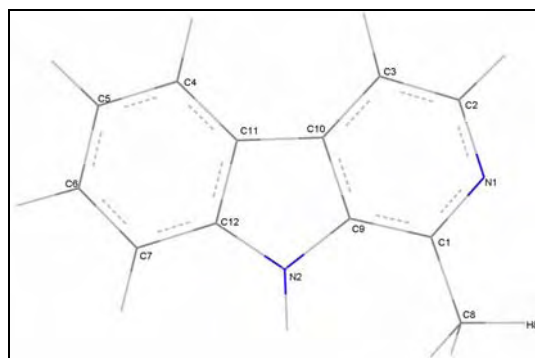


Fig. 1. The B3LYP/6-31+ G(d,p) optimized structure and the atom numbering of harmane

The calculated and experimental bond lengths and bond angles of harmane are summarized in Table 1 and Table 2, respectively. According to the crystal structure reported by El-Sayed et al. [10] there were two molecules of harmane in the unit cell, each hydrogen-bonded to the two others. All monomers in the unit cell had no significant differences in bond lengths and angles, therefore the experimental structural parameters of the neutral form of harmane summarized in Table 1 and Table 2 refer to the mean values of the molecular pair.

The crystallographic data revealed the planarity of the tricyclic harmane ring, which is in agreement with the calculated structure of harmane and the previously reported data [15].

**Table 1**  
The theoretically calculated and experimental bond angles (in [°]) for harmare free base

Angle	AM1	PM3	MNDO	HF/6-31G(d)	HF/6-31+G(d,p)	B3LYP/6-31G(d)	B3LYP/6-31+G(d,p)	Acta Cryst <sup>a</sup>	CCDB <sup>b</sup>
C12N2C9	107,12	106,08	107,05	108,92	108,92	109,35	109,24	107,25	108,15
C2N1C1	119,16	121,30	120,50	120,11	120,11	119,46	119,67	119,30	118,95
N1C1C9	120,21	118,40	118,87	119,65	119,66	119,72	119,60	119,50	120,00
N1C1C8	120,58	118,86	116,39	118,63	118,63	118,32	118,45	118,50	118,30
C9C1C8	119,21	122,76	124,74	121,71	121,71	121,95	121,95	122,05	121,75
N1C2C3	125,09	122,97	124,07	124,17	124,17	124,55	124,37	124,00	124,60
C2C3C10	117,07	117,13	117,30	117,05	117,05	117,30	117,31	116,40	117,05
C3C10C11	135,00	132,99	134,89	135,37	135,36	135,50	135,34	134,40	134,80
C3C10C9	118,67	119,75	118,28	118,09	118,10	117,72	117,81	119,35	118,40
C11C10C9	106,34	107,26	106,83	106,54	106,54	106,78	106,76	106,15	106,80
C10C11C4	133,70	132,47	134,16	133,90	133,91	134,05	134,01	133,75	134,05
C10C11C12	106,38	107,19	106,40	106,34	106,35	106,57	106,57	106,45	106,35
C4C11C12	119,92	120,34	119,44	119,75	119,75	119,38	119,42	119,75	119,65
C11C4C5	118,83	118,17	118,79	119,08	119,09	119,09	119,08	117,75	118,30
C4C5C6	121,09	121,25	121,18	120,40	120,39	120,71	120,69	121,75	121,30
C5C6C7	121,68	121,51	121,37	121,66	121,66	121,48	121,46	122,60	122,15
C6C7C12	117,87	117,45	117,50	117,59	117,58	117,60	117,61	115,70	116,95
C11C12N2	109,88	109,52	109,72	109,66	109,06	108,60	108,65	109,75	109,15

<sup>a</sup> Taken from Ref. [10]

<sup>b</sup> Taken from Ref. [11]

**Table 2**  
The theoretically calculated and experimental selected bond lengths (in Å) for harmane free base

Bond length	AM1	PM3	MNDO	HF/6-31G(d)	HF/6-31+G(d,p)	B3LYP/6-31G(d)	B3LYP/6-31+G(d,p)	Acta Cryst. <sup>a</sup>	CCDB <sup>b</sup>
N2C12	1,4107	1,4348	1,4213	1,3740	1,3740	1,3855	1,3865	1,3900	1,3785
N2C9	1,4076	1,4344	1,4221	1,3816	1,3815	1,3873	1,3886	1,3825	1,3740
N1C1	1,3527	1,3579	1,3583	1,3132	1,3132	1,3364	1,3375	1,3400	1,3210
N1C2	1,3468	1,3565	1,3531	1,3347	1,3348	1,3485	1,3502	1,3500	1,3495
C1C9	1,4153	1,4015	1,4166	1,3956	1,3956	1,4030	1,4040	1,3950	1,3935
C1C8	1,4916	1,4877	1,5073	1,5058	1,5059	1,5071	1,5066	1,5100	1,5020
C2C3	1,4076	1,3948	1,4118	1,3745	1,3745	1,3903	1,3915	1,3800	1,3750
C3C10	1,3870	1,3887	1,3999	1,3932	1,3933	1,3994	1,4009	1,3850	1,3915
C10C11	1,4523	1,4513	1,4622	1,4517	1,4518	1,4484	1,4489	1,4500	1,4300
C10C9	1,4467	1,4213	1,4410	1,3920	1,3919	1,4155	1,4159	1,4000	1,3965
C11C12	1,4468	1,4202	1,4405	1,4006	1,4006	1,4215	1,4222	1,4050	1,4085
C11C4	1,3879	1,3897	1,4052	1,3933	1,3934	1,4009	1,4023	1,4150	1,4045
C4C5	1,3943	1,3897	1,4053	1,3771	1,3771	1,3908	1,3926	1,3800	1,3745
C5C6	1,3992	1,3985	1,4123	1,4008	1,4008	1,4075	1,4093	1,3800	1,3825
C6C7	1,3930	1,3895	1,4049	1,3774	1,3774	1,3918	1,3935	1,3950	1,3845
C7C12	1,3983	1,3931	1,4072	1,3927	1,3927	1,3979	1,3993	1,4000	1,3940

<sup>a</sup> Taken from Ref. [10]

<sup>b</sup> Taken from Ref. [11]

All applied theoretical methods predicted structural rigidity and planarity of harmane ring. The orientation of methyl group in the harmane ring, which can be determined by the value of N1C1C8H8 dihedral angle was calculated to be  $-2,57^\circ$  (AM1 method) and  $-9,89^\circ$  (PM3 method) for neutral form of harmane. For cationic form of harmane the results of AM1 and PM3 calculations showed that the conformations in which the N1C1C8H8 angle was equal to  $0^\circ$  represented the minimum on the potential energy surface. The MNDO, HF and B3LYP calculations predicted that the structure in which N1C1C8H8 angle was equal to  $0^\circ$  for both neutral and monocationic form was identified as the energy minimum.

From the comparison of experimental structural parameters of harmane from Cambridge Crystallographic Database [11] with those obtained by El-Sayed and co-workers [10] it may be seen that the largest differences in the X-ray determined bond lengths and angles are observed for the C6C7C12 angle and the C10C11 bond (Fig. 2).

Therefore we made an assumption that if the deviations between crystallographic data and the theoretically calculated structural parameters are less than  $1,3^\circ$  and  $0,02 \text{ \AA}$  for bond angles and bond lengths, respectively, the theoretically determined structure of harmane is quite accurate. Fig. 3 and Fig. 4 show the differences between crystallographic data of harmane and the calculated geometrical parameters of  $\beta$ -carboline.

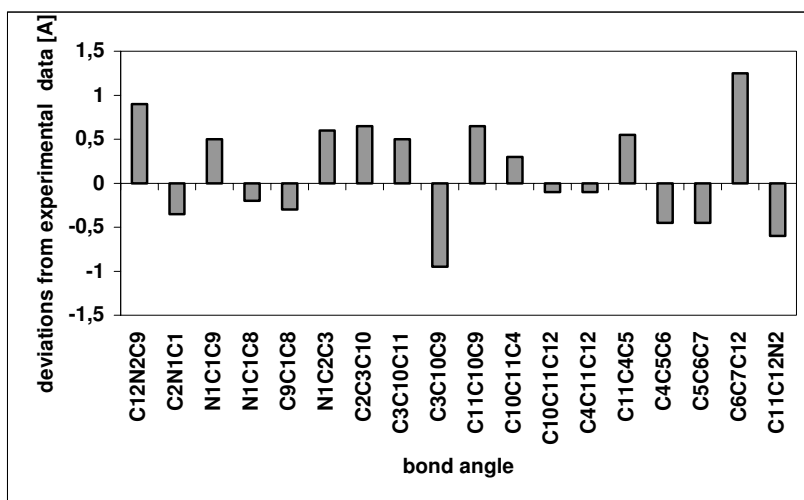


Fig. 2. Differences between crystallographic data taken from Cambridge Crystallographic Database [11] and those obtained by El-Sayed and coworkers [10]

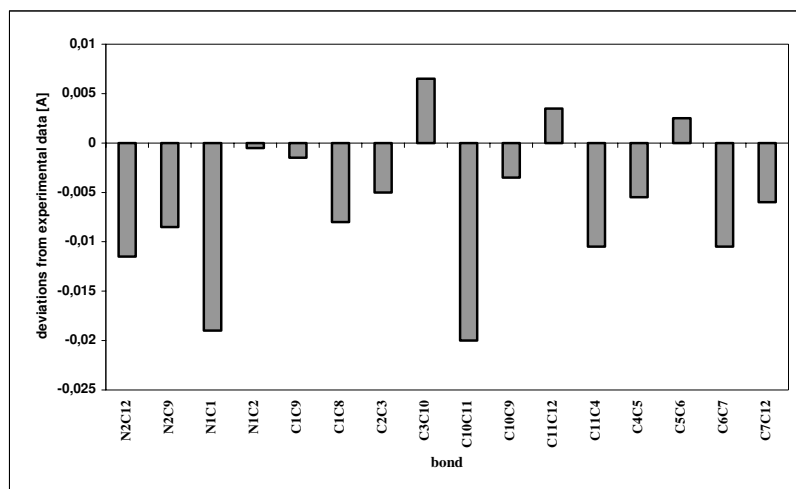


Fig. 2 (cd.). Differences between crystallographic data taken from Cambridge Crystallographic Database [11] and those obtained by El-Sayed and coworkers [10]

From the comparison of the calculated and the experimental structural parameters of neutral form of harmane (Table 3) it can be seen that the largest differences between the experimental and the calculated bond lengths is about -0,05 Å for semi-empirical methods and about -0,02 Å for both HF and B3LYP methods. The largest deviations between experimental and calculated bond angles is about 2,5° for the semi-empirical methods and about 1° for both HF and B3LYP methods. In general it should be noticed that the semi-empirical methods gave results less consistent with the crystallographic data. On the contrary, the bond lengths calculated by the HF and the B3LYP methods were in good agreement with the experimental data.

**Table 3**

The maximum differences between crystallographic [11] and theoretically calculated parameters of harmane

METHOD	BOND LENGTH[Å]		BOND ANGLE [°]	
AM1	-0,0502	C10C9	+2,54; -2,28	C9C1C8; N1C1C8
PM3	-0,0604	N2C9	-2,34; -2,07	C2N1C1; C12N2C9
MNDO	-0,0481	N2C9	-2,99; -1,91	C9C1C8; N1C1C8
HF/6-31G(d)	-0,0217	C10C11	-1,16	C2N1C1
HF/6-31+G(d,p)	-0,0218	C10C11	-1,16	C2N1C1
B3LYP/6-31G(d)	-0,0250	C10C9	-1,20	C12N2C9
B3LYP/6-31+G(d,p)	-0,0268	C5C6	-1,09	C12N2C9

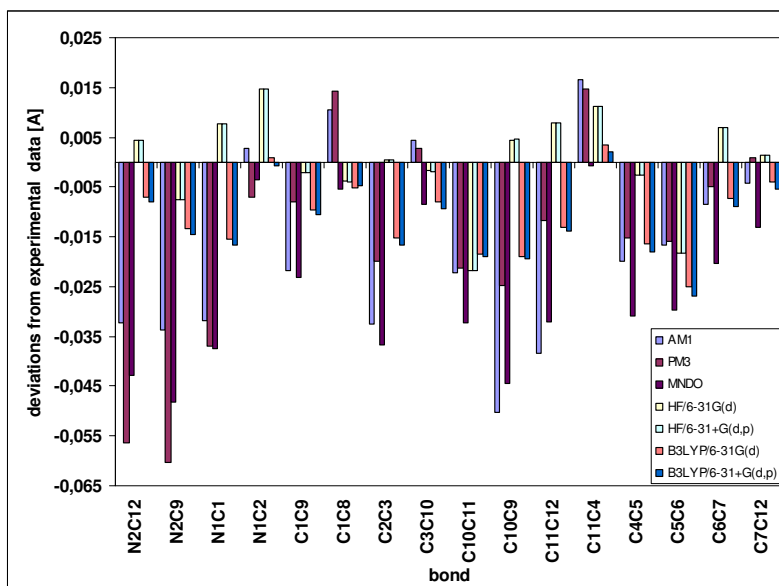


Fig. 3. Deviations between crystallographic data (bond lengths) from Cambridge Crystallographic Database [11] and those obtained from theoretical calculations

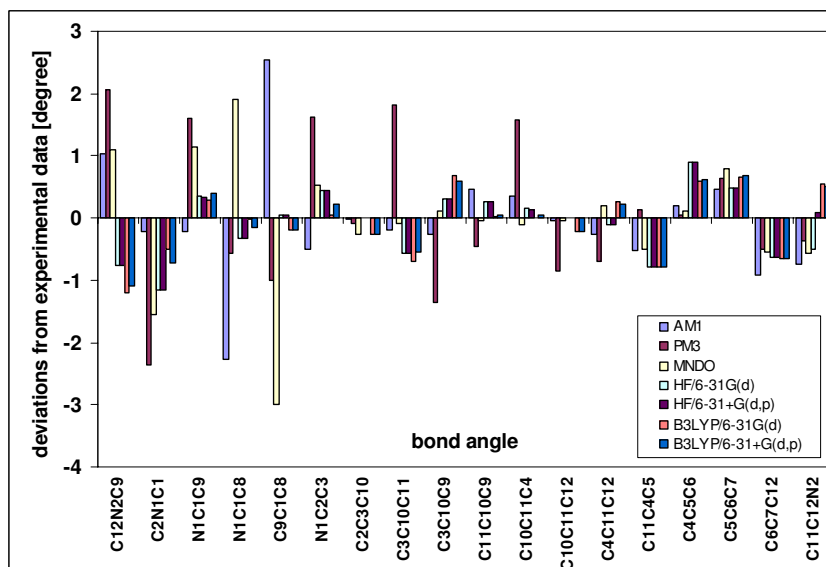


Fig. 4. Deviations between crystallographic data (bond angles) from Cambridge Crystallographic Database [11] and those obtained from theoretical calculations

### 3.2. Structural parameters of harmane monocation

In order to determine the changes in the geometrical parameters of harmane produced by the protonation process, the geometry optimization of harmane monocation was also carried out. The optimized structural parameters of harmane monocation are collected in Table 4 and 5.

Fig 5 shows the changes in the main geometrical parameters of harmane produced by the protonation process of the pyridinic nitrogen. As expected, the pyridinic fragment of the molecule shows the most significant variations in bond angles. The protonation process produces a decrease in the C2N1C1 bond angle (about  $-3,42^\circ$  for AM1,  $-2,05^\circ$  for PM3,  $-4,43^\circ$  for MNDO, about  $-4,84^\circ$  for HF and  $-5,69^\circ$  for B3LYP). The neighbouring angles: N1C2C3 and N1C1C9 increase ( $+2,95^\circ$  and  $+2,72^\circ$  for AM1,  $+1,75^\circ$  and  $+1,74^\circ$  for PM3,  $+3,55^\circ$  and  $+3,79^\circ$  for MNDO, about  $+3,53^\circ$  and  $+3,64^\circ$  for HF, and about  $4,24^\circ$  and  $+4,21^\circ$  for B3LYP). As far as the changes in bond lengths are concerned it should be noted that the general effect of the protonation process is to increase the C2C3 bond length and to decrease the N1C2 and N1C1 bond lengths (C2C3 is lengthened about  $+0,012\text{Å}$  AM1,  $+0,005\text{ Å}$  PM3, about  $0,015\text{ Å}$  for MNDO, HF and B3LYP). The magnitude of the N1C2 and N1C1 decrease is predicted to be  $-0,021\text{ Å}$  and about  $-0,018\text{ Å}$  for AM1 and PM3,  $-0,030$  and  $-0,026\text{ Å}$  for MNDO, about  $-0,018$  and  $-0,030\text{ Å}$  for HF, about  $-0,017$  and  $-0,024\text{ Å}$  for B3LYP. As predicted by HF and B3LYP calculations the geometrical parameters of the indole ring after protonation are slightly distorted from those corresponding to the neutral molecule (the C12N2C9 angle increases about  $+0,2^\circ$  and  $+0,13^\circ$  at the HF and the B3LYP level of theory, respectively). On the contrary, the semi-empirical methods predict that the C12N2C9 bond angle decreases upon protonation process, the magnitude of the decrease in C12N2C9 bond angle is calculated to be  $-0,99^\circ$  for AM1,  $-2,12^\circ$  for PM3 and  $-2,58^\circ$  for MNDO method. The rest of structural parameters of the indole fragment of harmane molecule are alternatively lengthened or shortened (Table 6 and 7).

**Table 4**  
The theoretically calculated bond angles (in [°]) for harmame monocation

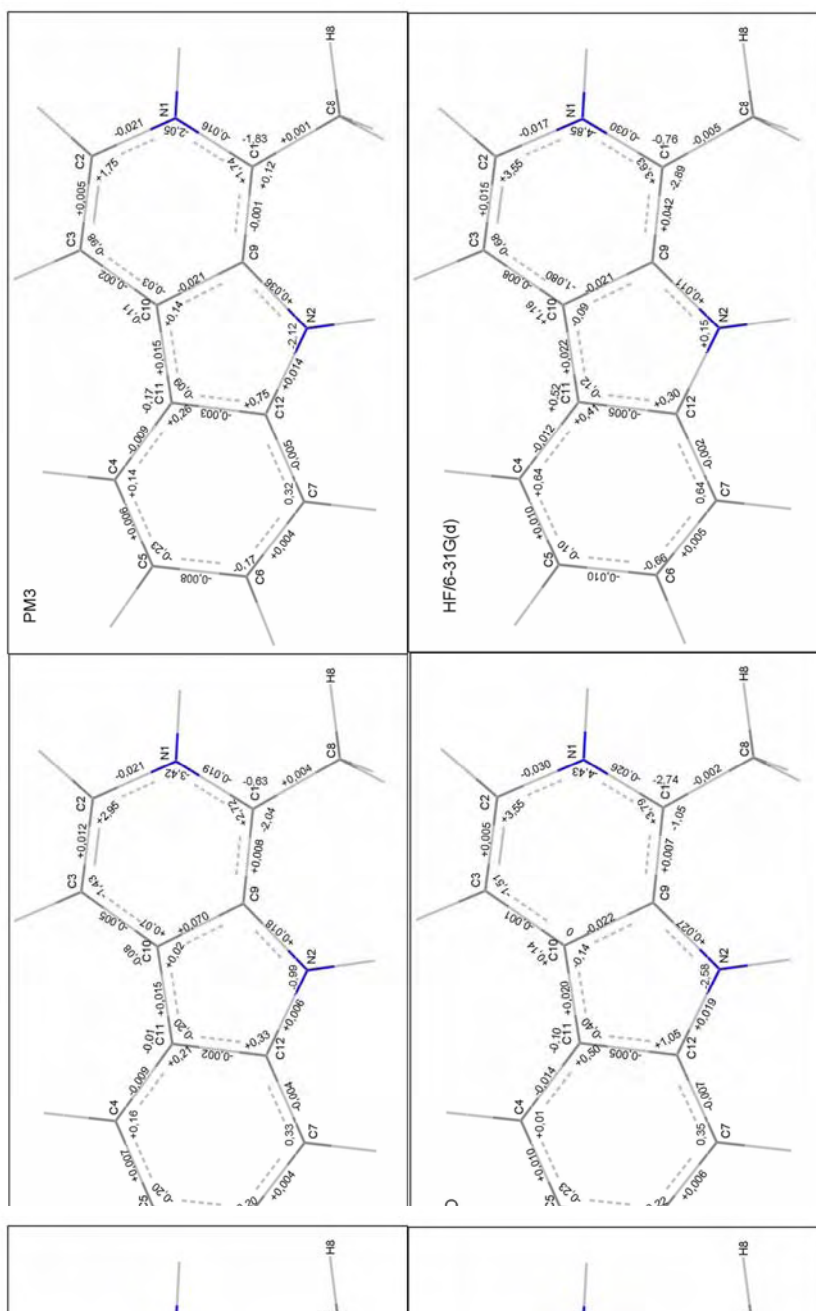
Angle	AM1	PM3	MNDO	HF/6-31G(d)	HF/6-31+G(d,p)	B3LYP/6-31G(d)	B3LYP/6-31+G(d,p)
C12N2C9	108,11	108,20	109,63	108,77	108,67	109,21	109,13
C2N1C1	122,58	123,35	124,93	124,96	124,94	125,24	125,26
N1C1C9	117,49	116,66	115,08	116,02	116,01	115,45	115,46
N1C1C8	121,25	120,69	119,13	119,39	119,39	119,50	119,48
C9C1C8	121,25	122,64	125,79	124,60	124,60	125,05	125,06
N1C2C3	122,14	121,22	120,52	120,62	120,66	120,22	120,22
C2C3C10	118,50	118,11	118,81	117,73	117,68	118,39	118,34
C3C10C11	135,08	133,10	134,75	134,21	134,19	134,49	134,46
C3C10C9	118,60	119,78	118,28	119,17	119,19	118,76	118,82
C11C10C9	106,32	107,12	106,97	106,63	106,63	106,74	106,72
C10C11C4	133,71	132,64	134,26	133,38	133,38	133,65	133,64
C10C11C12	106,58	107,28	106,80	106,46	106,44	106,61	106,61
C4C11C12	119,71	120,08	118,94	120,16	120,19	119,74	119,76
C11C4C5	118,67	118,03	118,78	118,44	120,19	118,41	118,41
C4C5C6	121,29	121,48	121,41	120,50	120,51	120,91	120,90
C5C6C7	121,88	121,68	121,59	122,32	122,29	121,30	121,96
C6C7C12	117,54	117,13	117,15	116,95	116,96	116,96	116,99
C11C12N2	109,55	108,77	108,67	109,36	109,43	108,78	108,82

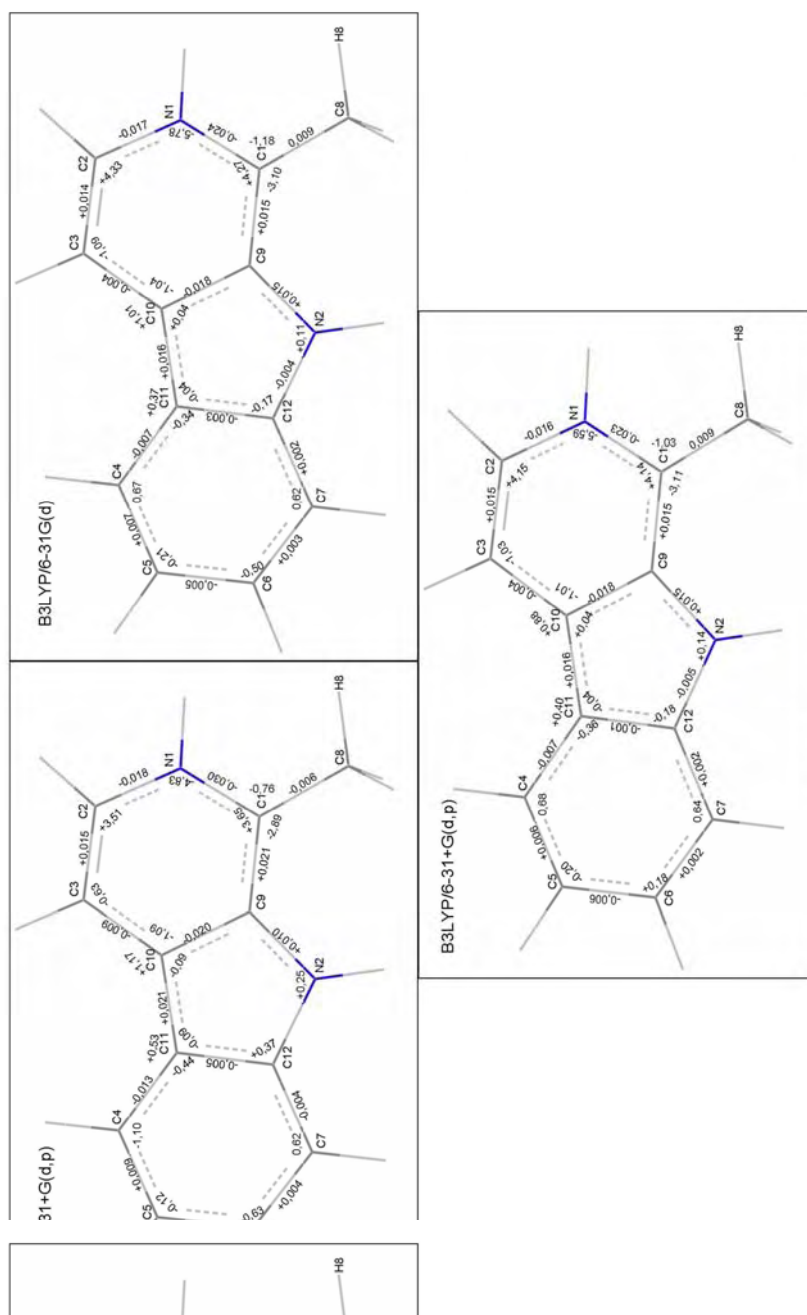
**Table 5**  
The theoretically calculated selected bond lengths (in [Å]) for harmene monocation

Bond length	AM1	PM3	MNDO	HF/6-31G(d)	HF/6-31G+(d,p)	B3LYP/6-31G(d)	B3LYP/6-31+G(d,p)
N2C12	1,4049	1,4210	1,4027	1,3740	1,3742	1,3901	1,3909
N2C9	1,3898	1,3982	1,3949	1,3706	1,3717	1,3722	1,3735
N1C1	1,3720	1,3736	1,3844	1,3427	1,3422	1,3602	1,3606
N1C2	1,3676	1,3772	1,3832	1,3512	1,3523	1,3650	1,3658
C1C9	1,4075	1,4026	1,4096	1,3535	1,3749	1,3881	1,3889
C1C8	1,4874	1,4868	1,5090	1,5012	1,5004	1,4986	1,4978
C2C3	1,3959	1,3895	1,3976	1,3595	1,3598	1,3762	1,3770
C3C10	1,3921	1,3911	1,4099	1,4010	1,4023	1,4034	1,4045
C10C11	1,4377	1,4364	1,4418	1,4300	1,4304	1,4323	1,4331
C10C9	1,4639	1,4420	1,4631	1,4127	1,4121	1,4335	1,4336
C11C12	1,4489	1,4230	1,4452	1,4011	1,4011	1,4221	1,4225
C11C4	1,3973	1,3987	1,4195	1,4048	1,4061	1,4078	1,4089
C4C5	1,3873	1,3834	1,3951	1,3669	1,3679	1,3842	1,3857
C5C6	1,4069	1,4065	1,4249	1,4110	1,4126	1,4131	1,4144
C6C7	1,3895	1,3853	1,3988	1,3726	1,3733	1,3896	1,3909
C7C12	1,4018	1,3978	1,4141	1,3950	1,3967	1,3964	1,3977

**Table 6**  
The geometrical parameter changes (in bond angles) of harmane produced by protonation process

Angle	AM1	PM3	MNDO	HF/6-31G(d)	HF/6-31+G(d,p)	B3LYP/6-31G(d)	B3LYP/6-31+G(d,p)
C12N2C9	-0,99	-2,12	-2,58	0,15	0,25	0,14	0,11
C2N1C1	-3,42	-2,05	-4,43	-4,85	-4,83	-5,78	-5,59
N1C1C9	2,72	1,74	3,79	3,63	3,65	4,27	4,14
N1C1C8	-0,67	-1,83	-2,74	-0,76	-0,76	-1,18	-1,03
C9C1C8	-2,04	0,12	-1,05	-2,89	-2,89	-3,1	-3,11
N1C2C3	2,95	1,75	3,55	3,55	3,51	4,33	4,15
C2C3C10	-1,43	-0,98	-1,51	-0,68	-0,63	-1,09	-1,03
C3C10C11	-0,08	-0,11	0,14	1,16	1,17	1,01	0,88
C3C10C9	0,07	-0,03	0	-1,08	-1,09	-1,04	-1,01
C11C10C9	0,02	0,14	-0,14	-0,09	-0,09	0,04	0,04
C10C11C4	-0,01	-0,17	-0,1	0,52	0,53	0,4	0,37
C10C11C12	-0,2	-0,09	-0,4	-0,12	-0,09	-0,04	-0,04
C4C11C12	0,21	0,26	0,5	-0,41	-0,44	-0,36	-0,34
C11C4C5	0,16	0,14	0,01	0,64	-1,1	0,68	0,67
C4C5C6	-0,2	-0,23	-0,23	-0,1	-0,12	-0,2	-0,21
C5C6C7	-0,2	-0,17	-0,22	-0,66	-0,63	0,18	-0,5
C6C7C12	0,33	0,32	0,35	0,64	0,62	0,64	0,62
C11C12N2	0,33	0,75	1,05	0,3	-0,37	-0,18	-0,17





5. Main geometrical parameter changes produced by pyridinic nitrogen protonation of harmanc. A minus sign means a decrease of the parameter value in the protonated form. Bond lengths in Å and bond angles in degrees[°]

**Table 7**  
The geometrical parameter changes (in bond lengths) of harmine produced by protonation process

Bond length	AM1	PM3	MNDO	HF/6-31G(d)	HF/6-31G+(d,p)	B3LYP/6-31G(d)	B3LYP/6-31+G(d,p)
N2C12	0,0058	0,0138	0,0186	0	-0,0002	-0,0045	-0,0044
N2C9	0,0178	0,0362	0,0272	0,011	0,0098	0,0151	0,0151
N1C1	-0,0193	-0,0157	-0,0261	-0,0295	-0,029	-0,0238	-0,0231
N1C2	-0,0208	-0,0207	-0,0301	-0,0165	-0,0175	-0,0165	-0,0156
C1C9	0,0078	-0,0011	0,007	0,0421	0,0207	0,0149	0,0151
C1C8	0,0042	0,0009	-0,0017	0,0046	0,0055	0,0085	0,0088
C2C3	0,0117	0,0053	0,0142	0,015	0,0147	0,0141	0,0145
C3C10	-0,0051	-0,0024	-0,01	-0,0078	-0,009	-0,004	-0,0036
C10C11	0,0146	0,0149	0,0204	0,0217	0,0214	0,0161	0,0158
C10C9	-0,0172	-0,0207	-0,0221	-0,0207	-0,0202	-0,018	-0,0177
C11C12	-0,0021	-0,0028	-0,0047	-0,0005	-0,0005	-0,0006	-0,0003
C11C4	-0,0094	-0,009	-0,0143	-0,0115	-0,0127	-0,0069	-0,0066
C4C5	0,007	0,0063	0,0102	0,0102	0,0092	0,0066	0,0069
C5C6	-0,0077	-0,008	-0,0126	-0,0102	-0,0118	-0,0056	-0,0051
C6C7	0,0035	0,0042	0,0061	0,0048	0,0041	0,0022	0,0026
C7C12	-0,0035	-0,0047	-0,0069	-0,0023	-0,004	0,0015	0,0016

### 3.3. Electronic properties of harmane

As can be seen from the comparison of data collected in Table 8, the HF, B3LYP calculated dipole moment of neutral form of harmane is higher in comparison with that predicted at the semi-empirical level. On the other hand, the MNDO calculated dipole moment is in good agreement with the value obtained by STO-3G molecular orbital calculations [15].

**Table 8**

The calculated dipole moments ( $\mu$ ) and HOMO-LUMO energy gap ( $\Delta E$ ) for the free base and the cationic form of harmane

	Neutral form				Cationic form			
	$\mu^*$ [ D ]	HOMO [ eV ]	LUMO [ eV ]	$\Delta E$ [ eV ]	$\mu$ [ D ]	HOMO [ eV ]	LUMO [ eV ]	$\Delta E$ [ eV ]
AM1	2,383	-8,550	-0,378	8,172	6,320	-12,272	-5,188	7,084
PM3	2,267	-8,617	-0,557	8,060	6,552	-12,241	-5,332	6,909
MNDO	2,425	-8,688	-0,578	8,110	5,849	-12,237	-5,406	6,831
HF/6-31G(d)	2,752	-7,725	2,635	10,360	6,355	-11,679	-2,381	9,298
HF/6-31+G(d,p)	2,806	-7,899	1,556	9,455	6,513	-11,727	-2,698	9,029
B3LYP/6-31G(d)	2,792	-5,625	-0,983	4,642	5,803	-9,640	-5,809	3,831
B3LYP/6-31+G(d,p)	2,899	-5,939	-1,386	4,553	5,918	-9,830	-6,020	3,811

\*the experimentally obtained dipole moment of harmane dissolved in 1,4-dioxane at 25°C is  $\mu^{\text{exp}}=3,36$  D [21]

According to the independent-particle model, it can be assumed that the excitation energy to the lowest excited singlet state of a molecule may be approximate by the energy difference between the HOMO and the LUMO orbital [22]. Therefore the energies of harmane HOMO and LUMO orbitals were calculated. The excitation energy corresponding to the long-wavelength absorption band of harmane was determined to be 3,757-3,646 eV in cyclohexane and about 3,351 eV in HCl-acidified water solution [16]. It should be noted that the semi-empirical and HF methods overestimate the values of HOMO/LUMO energies because of the negligence of electron correlation. The best results were obtained using the B3LYP method, in which the correlation energy is treated only semi-empirically. Including diffuse function into the B3LYP calculations had little effect on the predicted geometrical parameters of harmane (Table 1-4) but it improved the values of HOMO and LUMO orbital energies. The B3LYP/6-31+G(d,p) predicted electronic properties of harmane are the most consistent with experimental data.

### 3.4. The ZINDO-1 and TD B3LYP/6-31+G(d,p) predicted electronic transitions to the lowest excited singlet states of harmane

The absorption spectra of neutral form of harmane (in cyclohexane) is constituted of three bands. Two of them are strong and situated at  $\sim 240$  nm (5,166 eV) and  $\sim 286$  nm (4,335 eV), whereas the third band is weak and consists of two peaks around 330 (3,757 eV) and 340 nm (3,646 eV), respectively. In solutions, in low pH value harmane can exist in the form of monocation, in which the pyridinic nitrogen is protonated. The protonation of the pyridinic nitrogen results in the drastic change of the absorption spectra of harmane, which reflects the electronic properties of a molecule. In the absorption spectrum of harmane dissolved in HCl- acidified solutions four bands may be identified. The maxima of these bands are situated at  $\sim 204$  nm (6,077 eV),  $\sim 250$  nm (4,959 eV),  $\sim 300$  nm (4,133 eV) and  $\sim 370$  nm (3,351 eV), respectively. All observed bands result from  $\pi \rightarrow \pi^*$  transitions [16].

In order to find a theoretical model which can be useful in the interpretation of the absorption spectra of harmane, the ZINDO-1 semi-empirical as well as TD/B3LYP/6-31+G(d,p) calculations *in vacuo* were performed. The calculations were carried out on the B3LYP/6-31+G(d,p) optimized structure of harmane for neutral and monocationic form, because this method proved to be useful in the description of structural and electronic properties of the molecule under study. The theoretically predicted energies and oscillator strengths of electronic transitions to the lowest excited singlet states of harmane are presented in Table 9.

**Table 9**

Transition energies (E [eV]), wavelengths ( $\lambda$  [nm]) and oscillator strengths (f) of electronic transitions for harmane calculated using ZINDO-1 and TD B3LYP/6-31+G(d,p) methods *in vacuo*

	Neutral form				Cationic form			
	ZINDO-1		TD (B3LYP)/6-31+G(d,p)		ZINDO-1		TD (B3LYP)/6-31+G(d,p)	
	E [eV] $\lambda$ [nm]	f						
S <sub>1</sub>	3,820 324,6	0,1247	3,961 312,5	0,0723	3,245 381,9	0,1735	3,256 380,8	0,0407
S <sub>2</sub>	4,153 298,5	0,1380	4,561 271,8	0,0723	3,553 348,9	0,4197	3,940 314,7	0,1648
S <sub>3</sub>	4,285 289,3	0,0101	4,613 268,8	0,0020	4,254 291,4	0,0216	4,747 261,2	0,4652
S <sub>4</sub>	4,501 275,4	0,0290	4,884 253,9	0,0009	4,670 265,5	0,7088	4,805 258,0	0,0443
S <sub>5</sub>	4,948 250,6	1,2082	5,176 239,6	0,2042	4,761 260,4	0,1460	5,120 242,2	0,0651

Before we make a brief comment on the comparison of experimental and calculated properties of electronic transitions in harmane, we should emphasize that no solvent effects were taken into account in the calculation. Therefore we should not expect the excellent quantitative correlation of experimental and calculated properties of electronic transitions. Bearing that in mind we may say that the ZINDO-1 method, despite its simplicity, gives quite good qualitative description of electronic transition in neutral harmane. The energy of  $S_1$  transition is larger only by 0,063 eV compared with the experimental value of 3,757eV. The  $S_2$ ,  $S_3$  and  $S_4$  states might originate from experimental band of the energy 4,335 eV (286 nm). The  $S_3$  and  $S_4$  states were expected to be less strong (based on its oscillator strength) making it likely that the peak corresponding to the  $S_2$  would obscure the ones arising from the  $S_3$  and  $S_4$  states. Comparing the experimental and the calculated energies of electronic transitions in neutral form of harmane it should be noted that the TD (B3LYP)/6-31+G(d,p) calculated energy of the electronic transition to the lowest excited singlet state of harmane is overestimated, that is too large by about 0,315 eV compared with their experimental value. That may be attributed to the wrong long-range behavior of TD B3LYP exchange-correlation functional, since it decays faster than  $1/r$ , where  $r$  is the electron-nucleous distance. As a result TD B3LYP method has severe problems with the correct description of Rydberg states and extended  $\pi$ -systems [23]. As far as cationic form of harmane is concerned, both the ZINDO-1 and TD B3LYP/6-31+G(d,p) methods underestimated the energies of the two lowest electronic transitions. The calculations suggest that the lowest singlet excited state of harmane cation originated from the two close lying  $S_1$  and  $S_2$  transitions. Moreover the calculated using above mentioned methods ground to excited state transition electric dipole moment is evidently larger for  $S_2$  as compared with the value calculated for  $S_1$  state. That makes the  $S_2$  state more sensitive to polar environment. Due to solvent stabilization of the  $S_2$  state, it is possible that the  $S_1$  and  $S_2$  states might interchange and the  $S_2$  state would become the lowest-lying excited state. Therefore it is important to consider solvent effects in the prediction of the electronic transitions in harmane.

#### 4. Conclusions

In the current work the geometry optimization of both the neural and cationic form of harmane with the use of semi-empirical, Hartree-Fock and B3LYP theories were performed. The calculated structural and electronic properties of harmane were compared with the experimental data in order to select the theoretical approach which gives the most accurate description of electronic structure of harmane molecule. In conclusion, from all studied method e.g., AM1, PM3, MNDO, HF and B3LYP, the B3LYP calculations seemed to give the most accurate description of the electronic structure for both neutral and

cationic forms of harmane. Therefore, the electronic structure of harmane predicted by B3LYP/6-31+G(d,p) was used for further ZINDO-1 and TD (B3LYP)/6-31+G(d,p) calculations in order to estimate the properties of electronic transitions in harmane. The calculations revealed that including solvent effects in the theoretically predicted electronic transitions of harmane is crucial. The most popular models to examine the influence of solvent are Polarized Continuum Model (PCM) (which is available for TD B3LYP calculations) and the semi-empirical SM5.4 continuum solvent model. Therefore the semi-empirical AM1-CI and PM3-CI calculations with SM5.4 solvation model as well as the TD/6-31+G(d,p) PCM calculations for harmane have been performed [24,25].

**Acknowledgements.** Financial support from the State Committee for Scientific Research (Grant No. 3T08E06327) is gratefully acknowledged. A. Kowalska is a grant holder of "Mechanizm WIDDOK" project supported by European Social Fund and Polish State (contract number Z/2.10/II/2.6/04/05/U/2/06).

## References

- [1] **Muñoz M.A., Carmona C., Hidalgo J., Guardado P., Balón M.:** Molecular associations of flavins with betacarbolines and related indoles. *Bioorg. Med. Chem.*, **3**, 41-47, (1995).
- [2] **Herraiz T., Chaparro C.:** Human monoamine oxidase enzyme inhibition by coffee and  $\beta$ -carbolines norharman and Harman isolated from coffee. *Life Sciences*, **78**, 795-802, (2006).
- [3] **Anderson N.J., Tyacke R.J., Husbands S.M., Nutt D.J., Hudson A.L., Robinson E.S.J.:** In vitro and ex vivo distribution of [ $^3\text{H}$ ]harmane, an endogenous  $\beta$ -carboline, in rat brain. *Neuropharm.*, **50**, 269-276, (2006).
- [4] **Spijkerman R., van den Eijnden R., van de Mheen D., Bongers I., Fekkes D.:** The impact of smoking and drinking on plasma levels of norharman, *European Neuropsychopharm.*, **12**, 61-71, (2002).
- [5] **Muñoz M.A., Guardado P., Galán M., Carmona C., Balón M.:** A spectroscopic study of the molecular interactions of harmane with pyrimidine and other diazines. *Biophys. Chem.*, **83**, 101-109, (2000).
- [6] **Balón M., Muñoz M.A., Carmona C., Guardado P., Galán M.:** A fluorescence study of the molecular interactions of harmane with the nucleobases, their nucleosides and mononucleotides. *Biophys. Chem.*, **80**, 41-52, (1999).
- [7] **Balón M., Carmona C., Guardado P., Muñoz M.A.:** Hydrogen-bonding and proton transfer interactions between harmane and trifluoroethanol in the ground and excited singlet states. *Photochem. Photobiol.*, **67**, 414-419, (1998).
- [8] **Carmona C., Galán M., Angulo G., Muñoz M.A., Guardado P., Balón M.:** Ground and singlet excited state hydrogen bonding interactions of betacarbolines. *Phys. Chem. Chem. Phys.*, **2**, 5076-5083, (2000).

- [9] **de Souza J.M., dos Anjos P.N.M., de Azevedo W.M., Marques A.S.:** Long-lived emission at room temperature of harmane dispersed in poly(acrylic acid)-poly(vinyl alcohol) polymer network. *J. Luminescence*, **81**, 225-229, (1999).
- [10] **El-Sayed K., Barnhart D.M., Ammon H.L., Wassel G.M.:** Structure of harman,1-methyl-9H-pyrido[3,4-b]indole. *Acta Cryst., C*, **42**, 1383-1385, (1996);
- [11] Cambridge Crystallographic Database, <http://www.ccdc.cam.ac.uk>
- [12] **Cramer C.J.:** Essentials of computational chemistry. Theories and Models. Wiley, (2006).
- [13] **Hidalgo J., Balón M., Carmona C., Muñoz M.A., Pappalardo R.R.:** AM1 study of a  $\beta$ -carboline set: structural properties and potential reactivity. *J.Chem. Soc. Perkin Trans 2*, 65-71, (1990).
- [14] **Muñoz M.A., Balón M., Hidalgo J., Carmona C., Pappalardo R.R., Marcos E.S.:** AM1 study of a  $\beta$ -carboline set. Part III.: substituent effects. *J.Chem. Soc. Perkin Trans.2*, 1729-1734, (1991).
- [15] **Konschin H., Tylli H., Gynther J., Rouvinen J.:** The molecular structure of norharman and harman: an STO-3G molecular orbital investigation. *J. Mol. Struct.*, **153**, 307-321, (1987).
- [16] **Marques A.D.S., Souza H.F., Costa I.C., de Azevedo W.M.:** Spectroscopic study of harmane in micelles at 77 K using fluorescent probes. *J. Mol. Struct.*, **520**, 179-190, (2000).
- [17] **Tapia M.J., Reyman D., Vinas M.H., Arroyo A., Poyato J.M.L.:** An experimental and theoretical approach to the acid-base and photophysical properties of 3-substituted  $\beta$ -carbolines in aqueous solutions. *J. Photochem. Photobiol. A*, **156**, 1-7, (2003).
- [18] **Angulo G., Carmona C., Pappalardo R.R., Muñoz M.A., Guardado P., Marcos E.S., Balón M.:** An experimental and theoretical study on the prototropic equilibria of the four carboline isomers. *J. Org. Chem*, **62**, 5104-5109, (1997).
- [19] **Chou P., Liu Y., Wu G., Shiao M., Yu W.:** Proton-transfer tautomerism of  $\beta$ -carbolines mediated by hydrogen-bonded complexes. *J. Phys.Chem. B*, **105**, 10674-10683, (2001).
- [20] **Remko M., Swart M., Bickelhaupt M.:** Theoretical study of structure,  $pK_a$ , lipophilicity, solubility, absorption, and polar surface area of some centrally acting antihypertensives. *Bioorg. Med. Chem.*, **14**, 1715-1728, (2006).
- [21] **Isidro S., Monzo S., Codoñer A., Medina P., Olba A., Valero R.:** Apparent dipole moments and molar volumes of  $\beta$ -carbolines and carbazole in dioxane solution. *J. Chem. Soc. Perkin Trans II*, 261-263, (1988).
- [22] **Sadlej J.:** Obliczeniowe metody chemii kwantowej CNDO, INDO, NDDO, ab initio. Warszawa, PWN, (1988).
- [23] **Drew A., Head-Gordon M.:** Single-reference ab initio methods for the calculation of excited states of large molecules. *Chem. Rev.*, **105**, 4009-4037, (2005).
- [24] **Stobiecka A., Kowalska A., Wysocki S.:** Application of semi-empirical methods in the study of harmane solvatochromism. *PTChem.*, (2005).
- [25] **Kowalska A., Stobiecka A., Wysocki S.:** Structural and electronic properties of harmane monocation. Theoretical aspects. *PTChem.*, (2006).

## TEORETYCZNE BADANIA STRUKTURY I WŁAŚCIWOŚCI ELEKTRONOWYCH HARMANU

### Streszczenie

W pracy obliczono optymalizację struktury elektronowej harmanu z wykorzystaniem różnych metod obliczeniowych, tj. metod semi-empirycznych (AM1, PM3, MNDO), metody Hartree-Focka, jak również metody B3LYP. W celu sprawdzenia dokładności i użyteczności wyżej wymienionych metod teoretycznych w przewidywaniu struktury badanej  $\beta$ -karboliny obliczone parametry strukturalne harmanu porównano z dostępnymi w literaturze danymi krystalograficznymi. Następnie obliczono wybrane właściwości elektronowe neutralnej oraz kationowej formy harmanu.

Uzyskaną z obliczeń wartość różnicy energii orbitali HOMO i LUMO, którą można traktować jako przybliżoną energię przejścia do najniższego stanu singletowego cząsteczki, porównano z uzyskaną z eksperymentu wartością energii wzbudzenia harmanu. Spośród wykorzystanych w pracy metod obliczeniowych, zastosowanie metody B3LYP z użyciem bazy 6-31+G(d,p) pozwoliło na uzyskanie zadowalającego opisu właściwości strukturalnych i elektronowych harmanu. Dlatego też uzyskaną za pomocą tej metody strukturę elektronową harmanu wykorzystano do obliczeń energii przejść elektronowych cząsteczki. Obliczone metodą ZINDO-1 oraz TD B3LYP energie przejść elektronowych porównano z energią przejść elektronowych odpowiadającym odpowiednim pasmom w widmie absorpcji neutralnej oraz kationowej formy harmanu.

Instytut Podstaw Chemii Żywności  
Wydział Biotechnologii i Nauk o Żywności  
Politechnika Łódzka